Multilayered Stub Loaded-SIR for Compact Dual-BPF and Quad-channel Diplexer Design

Soaad L. AJEEL, Raaed T. HAMMED

Department of Electrical Engineering, University of Technology-Iraq, Baghdad, Iraq

souadlateaf@gmail.com, raaed.t.hammed@uotechnology.edu.iq

Submitted March 25, 2024 / Accepted August 7, 2024 / Online first October 31, 2024

Abstract. *This paper considers a novel design technique of compact dual-BPF and four-channel diplexer for a multi-service communication system. The suggested dual-band passband filter is constructed by a double-layered stub loaded-stepped impedance resonator (SL-SIR), leading to a tiny circuit area, and lightweight, low cost, and good characteristic performance. Herein, the SL-SIR resonant odd-mode is used to realize the first passband, while the resonant even-mode is used to realize the second passband. Also, the proposed three-port quad-channel diplexer is performed by two different double-layered dual-passband filters, which also have a very compact circuit area. For practical verification, a two-passband filter working at 2.5/4 GHz with a circuit area of 91.7 mm^2 and a four-channel diplexer working at 2.5/4 GHz and 3.5/5.2 GHz with a circuit area of 0.0639 λ_g^2 excluding feeding ports are designed, manufactured, and measured. The electromagnetic simulated and measured responses are compared and discussed. Obviously, the comparison shows good agreement improving the expected filtering response. The diplexer offers insertion/return losses of about (0.44/0.74) dB/(0.45/1.12) dB for channel 1/channel 2, and (21.30/21.72) dB/(19.81/20.54) dB for channel 3/channel 4.*

Keywords

Stub loaded-stepped impedance resonator, double-layered dual-BPF, four-channel diplexer, compact multi-channel diplexer, multilayered dual-PBF

1. Introduction

Recently, RF and microwave filters are widely investigated to meet the rapid requirements of modern wireless communication technologies [1–5]. For the purposes of integrated multi-wireless network systems, many dual-band BPFs and diplexers are developed using different techniques and structures to be fitted up with high IP/OP-passband performance [6–21]. To enhance a compact dual-band bandpass filter, a composite right-left handed structure is adopted in [6]. For the same purposes, [7] proposed a dual narrow band filter based on grounded stepped impedance resonator (SIR). On the contrary, [8] proposed a traditional open/short microstrip-stubs to design dual passband filter with wide bandwidth performance. Using a discriminating coupling technique in [9] and a parallel-coupled SIR in [10], dual-band BPFs are developed with high-selective characteristic performance. Furthermore, [11] introduced a dual-BPF with high-passbands isolation. In addition, a differential dual-band BPF with independently controllable passbands is investigated in [12]. In order to design full independently multi-filtering attitude, three-port diplexers are deeply studied based on single and dual BPFs [13–20]. Of them, two-channel diplexers are realized adopting different structures and techniques such as square open-loop resonators [13], complicated microstrip structure [14], based on synchronous and ansynchronous coupling [15] and multilayered U-shaped resonators [16]. Generally, quad-channel diplexers are designed based on dual-band bandpass filter [17–20]. With high isolation performance but large in size, four-channel diplexer is reported in [17]. Using a dual-mode resonator two dual-band BPFs are integrated to perform four-channel diplexer in [18]. However, the resulted diplexer has unequal fractional bandwidth (FBW). For compactness purposes, [19] and [20] developed a three-port four-channel diplexers based on quad-mode and quint-mode resonator respectively. Unfortunately, the proposed diplexers has either a random FBW or poor selectivity. Moreover, 6-channel diplexer is achieved in [21] based on multilayer technology. In addition, the reported works suffer from weak rejection band performance.

In this article, two new desirable dual-band BPFs are realized and parallelly coupled to develop quad-channel diplexer for a multiservice communication system. The dual-band BPF configuration is composed of stepped-impedance resonator SIR middlely-loaded by a low-impedance open stub. Each filter is analyzed and constructed based on multilayer technology. The filtering response is studied deeply using advanced design system (ADS) software program. Practically, the suggested dual-band BPF and the quad-channel diplexer are constructed using two (Rogers Ceramic RO4360) substrate that has a relative dielectric constant $\varepsilon_r = 6.15$ and a thickness $h = 0.508$ mm. The measurements of the prototypes are carried out using VNA and their responses are compared with the simulation results. The compared results show that the expected filtering responses are verified and the filters have good performance.

DOI: 10.13164/re.2024.0629

2. SL-SIR Design and Analysis

The layout configuration of the proposed dual-mode stub loaded-SIR is shown in Fig. 1(a). It consists of half-wave folded stepped impedance resonator loaded by a low-impedance open stub at its middle. In Fig. 1(a), the structure is described by (Y_1, Y_2, θ_1, θ_2, and θ_3). Due to the symmetry of the SL-SIR, its circuit and frequency response are analyzed based on even-odd analysis theory. Indeed, two equivalent circuits are considered to explain the odd/even-mode frequency response: Fig. 1(b) and Fig. 1(c), respectively.

Following the theoretical analysis stated in [21], the resonant condition of the odd-model circuit (f_{odd}), Fig. 1(b), can be calculated by:

$$\tan\theta_1 \cdot \tan\theta_2 = Y_1 / Y_2 = Z_2 / Z_1 = R_Z, \quad (1)$$

$$\theta_T = 2(\theta_1 + \theta_2) < \pi \quad (2)$$

where R_Z is the impedance ratio and θ refers to the resonator's angular length $\theta = \beta\ell$. Note that the resonant condition can be simply controlled by modifying the impedance ratio and the angular lengths θ_1 and θ_2. In the even-model circuit in Fig. 1(c), the structure can be also consider like a SIR and the resonant frequency response (f_{odd}) can be defined by:

$$\tan(\theta_1 / 2) \cdot \tan\theta_2 = Y_1 / Y_2 = Z_2 / Z_1 = R_Z, \quad (3)$$

$$\theta_T = (\theta_1 + 2\,\theta_2) < \pi\,. \quad (4)$$

In this case the impedance of the middle stub (Y_3/2) is equal to Y_2 and $\theta_3 = \theta_2$.

For the purposes of this work and to improve the aforementioned analysis, the suggested SL-SIR is designed to generate two resonance frequencies (2.5 and 4 GHz) using

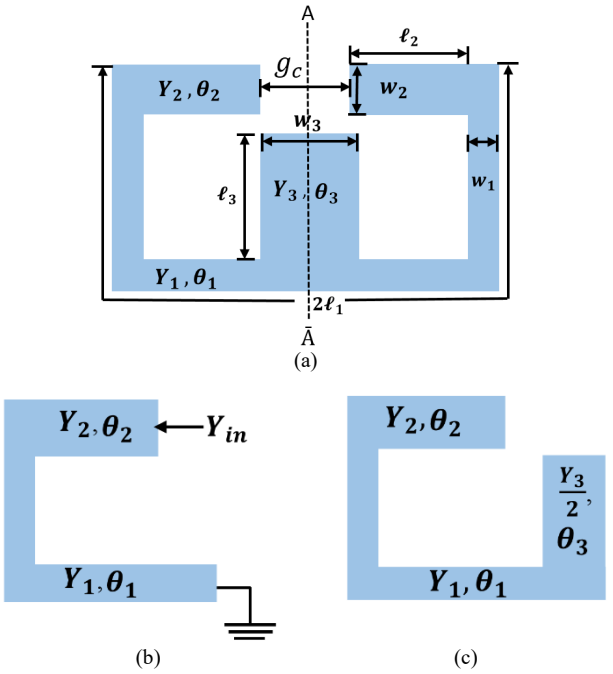

Fig. 1. (a) The basic layout configuration of the SL-SIR; (b) Odd-model circuit; (c) Even-model circuit.

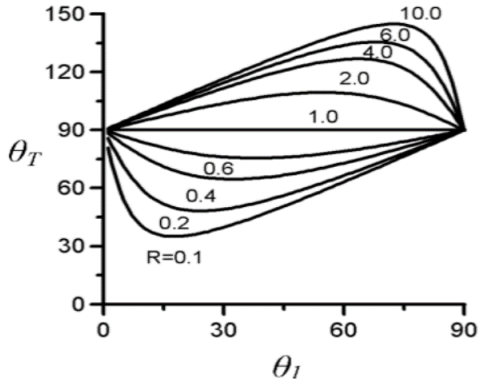

(a)

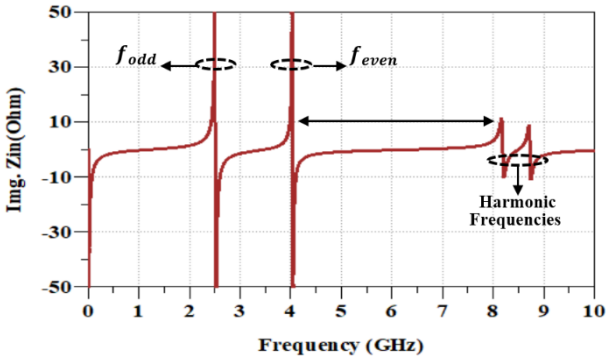

(b)

Fig. 2. ($\ell_1 = 9.3$ mm, $\ell_2 = 2.5$ mm, $\ell_3 = 3.5$ mm, $w_1 = 0.5$ mm, $w_2 = 1$ mm, $w_3 = 2$ mm and $g_c = 1$ mm) characteristic performance: (a) SIR resonance condition. (b) Imaginary frequency response of its input impedance, Fig. 1(a).

a Rogers Ceramic RO4360 substrate with a relative dielectric constant $\varepsilon_r = 6.15$ and a thickness $h = 0.508$ mm. Indeed, the impedance ratio R_Z is chosen to be 0.5 in which the line impedances of the SL-SIR are $Z_1 = 78\ \Omega$, $Z_2 = 39\ \Omega$ and $Z_3 = 19.5\ \Omega$. Utilizing the data base stated in [22], Fig. 2(a), the total angular length of the desired $f_{odd} = 2.5$ GHz is found out to be $\theta_T = 150°$ in which $\theta_1 = 54°$ and $\theta_2 = 21°$. In the same fashion, the specified $f_{even} = 4$ GHz is realized with a total angular length $\theta_T = 70°$ in which $\theta_1 = 28°$ and $\theta_2 = 21°$. To this end, the physical dimensions of the SL-SIR are obtained and its resonance attitude is simulated with aid of the advanced design system (ADS) simulator [23]. Figure 2(b) depicts the simulated imaginary part of the input impedance of the SL-SIR. Clearly, the desired f_{odd} and f_{even} are generated with wide range of high spurious frequencies elimination.

3. Circuit Design

3.1 A Novel Dual Band BPF

Based on the above analysis in Sec. 2, the SL-SIR is realized to produce two specified frequencies $f_{odd} = 2.5$ GHz and $f_{even} = 4$ GHz with very wide harmonics suppression response. Basically, these frequencies are the center frequencies of the desired first and second passbands. The conductor layout in the three dimension geometry and the coupling

mechanism block diagram of the proposed filter is shown in Fig. 3. On the grounded substrate, two identical SL-SIRs are magnetically coupled using a space coupling (S). The feature of this distance is to control the fractional bandwidth of the desired passbands. In order to obtain the filtering response, two IP/OP open stubs are performed on a second one-layer substrate and vertically integrated to the SL-SIRs, Fig. 3(a). Herein, the thickness of the second substrate (h_2) can adjust the required coupling strength and enhance the filtering attitude. Figure 3(b) easily explains the coupling mechanism and the signal path from the source to the load improving the dual-band filtering response.

In this example, 2.5/4 GHz dual-band BPF is implemented in which two of the SL-SIRs having the same physical dimensions, Fig. 2(b), are coupled through a coupling distance $S = 0.5$ mm using a grounded substrate with a dielectric constant $\varepsilon_{r1} = 6.15$ and thickness $h_1 = 0.508$ mm. Next, two input/output broadside coupled lines, Fig. 3(a), are patterned on a second one-layer substrate has a dielectric constant of $\varepsilon_{r2} = 6.15$ and thickness $h_2 = 0.508$ mm with physical lengths $\ell_{w1} = 0.3$ mm, $\ell_{w2} = 3$ mm. Finally, the broadside coupled lines are directly connected to 50-Ω I/O-stub ports of $w_p = 1.37$ mm and capacitively coupled to the bottom circuit, Fig. 3(a). Note that the coupling parameters S and h_2 are obtained based on the deep numerical analysis reported in [24]. With the aid of the ADS software, the desired dual-band filter is simulated and its results are illustrated in Fig. 4. Obviously, the coupling strength at the even-passband is very weak and need to be increased to improve the passband performance. Therefore, a short open-stub with optimum physical dimensions of $\ell_4 = 5$ mm and $w_4 = 1.6$ mm is created on the top substrate and located at the low-impedance stubs of the SL-SIRs, Fig. 5. Resimulating the modified filter circuit (Fig. 5), the even-passband is significantly enhanced as shown in Fig. 4. However the filter shows high skirt roll off, it has two good isolated passbands with 8% FBW at the odd-passband and 5% FBW at the even-passband. Also, the filter offers good passband performance of 0.43/0.55 dB insertion loss and 24.7/27.4 dB return loss with wide suppression characteristics exceeding 3.6 GHz at 20 dB attenuation. Moreover, the filter performance is verified with a circuit area about of 91.7 mm^2 without the feeding ports.

For practical achievement, a dual-band BPF working at 2.5/4 GHz is fabricated and measured. The fabricated circuit dimensions are listed in Tab. 1. A photograph pictures of the prototype before and after alignment are shown in Fig. 6(a) and (b), respectively. Consequently, the filter circuit is tested using an E5071C Vector Network Analyzer (VNA) and its measured responses are sketched and compared with simulated results in Fig. 6(c). The compared responses show good agreement and the filter has good filtering attitude covering a very compact circuit area less than 92 mm^2 excluding the feeding ports. However, the little shift in the measured results can be caused by the manufacturing process such as the crystal boned glue used for the circuit's alignment and alignment process. Irregardless, Table 2 exhibits the filter capabilities, when its specification are compared against the recent published works.

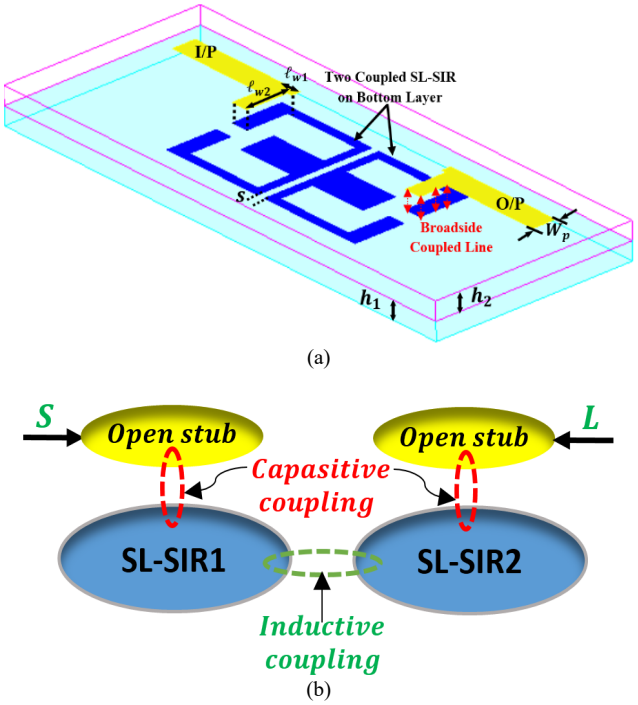

Fig. 3. The multi-layered SL-SIR dual-band BPF: (a) 3-D geometry of its conductor layout. (b) Coupling mechanism diagram.

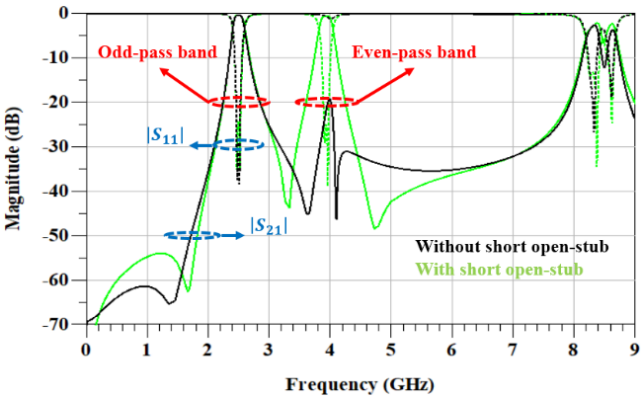

Fig. 4. The simulated $|S_{21}|/|S_{11}|$ magnitudes of the multi-layered SL-SIR dual-band BPF without modification and with modification, Fig. 3(a) and Fig. 5, respectively.

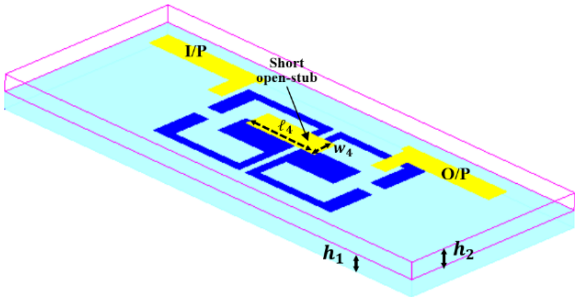

Fig. 5. The modified multi-layered SL-SIR dual-band BPF with short open-stub.

Substrate	Length (mm)	Width (mm)
Grounded substrate ε_{r1} = 6.15, h_1 = 0.508 mm	ℓ_1 = 9.3, ℓ_2 = 2.5, ℓ_3 = 3.5, g_c = 1, S = 0.5	w_1 = 0.5, w_2 = 1, w_3 = 2
Ungrounded substrate ε_{r2} = 6.15, h_2 = 0.508 mm	ℓ_{w1} = 0.3, ℓ_{w2} = 3, ℓ_4 = 5,	w_1 = 0.5, w_2 = 1, w_p = 1.37, w_4 = 1.6

Tab. 1. Physical dimensions of the double-layered SL-SIR DB-BPF, Fig. 1(a) and Fig. 2(a).

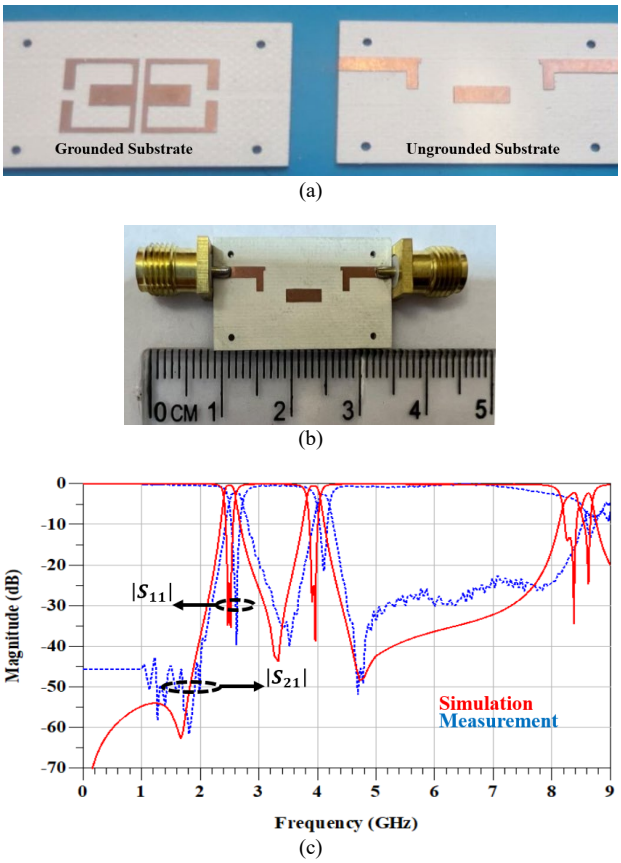

Fig. 6. The manufactured multi-layered SL-SIR dual-band BPF, Fig. 5: (a) Its photograph before alignment. (b) Its photograph after alignment. (c) Its simulation and measurement scattering-parameters $|S_{11}|$ and $|S_{21}|$.

3.2 Three-port Quad-channel Diplexer Design

A very compact dual-band BPF with high filtering response characteristics is developed and achieved based on a significant multi-layer design technique, Sec. 3.1. For the purposes of multiple-services communication systems, a three-port four-channel diplexer is designed and analyzed using two individual dual-band passband filters. Therefore, a second multi-layered SL-SIR dual-band passband filter working at 3.5/5.2 GHz is realized based on the design procedure stated in Sec. 3.1. Indeed, the filter layout dimensions are obtained and summarized in Tab. 3.

The simulation results, Fig. 7, show that the filter provides odd-FBW of 8% with insertion/return losses of 0.4/25.5 dB and even-FBW of 5% with insertion/return losses of 0.5/24.5 dB at 3.5/5.2 GHz. Besides, the filter structure is very small covering circuit area of about 56 mm^2. Next, the two constructed filters are gathered with one input port to perform the desired three-port quad-channel diplexer as shown in Fig. 8(a). In this figure, the two circuits are cascaded directly on the top-layer using one input feeding port. This leads to circuit's mismatch and affects the IP/OP broadside coupling. Therefore, the coupling lengths of the broadside open-stubs at the input and outputs of the diplexer circuit, Fig. 8(a), are slightly changed, and their final tuned lengths are summarized in Tab. 4. In the same table, the short open-stub dimensions for each filter are retuned to improve the even-passbands performance.

However, the diplexer layout signal path and its filtering attitude are explained using a coupling scheme diagram shown in Fig. 8(b). To this end, the diplexer is simulated and its results are sketched in Fig. 9. The simulation

Substrate	Length (mm)	Width (mm)
Grounded substrate ε_{r1} = 6.15, h_1 = 0.508 mm	ℓ_1 = 7.2, ℓ_2 = 1.5, ℓ_3 = 3.2, g_c = 1, S = 0.3	w_1 = 0.5, w_2 = 1, w_3 = 2
Ungrounded substrate ε_{r2} = 6.15, h_2 = 0.508 mm	ℓ_{w1} = 0.5, ℓ_{w2} = 2, ℓ_4 = 5	w_1 = 0.5, w_2 = 1, w_p = 1.37, w_4 = 1.6

Tab. 3. Physical dimensions of the 3.5/5.2 GHz double-layered SL-SIR DB-BPF.

Ref.	Frequency (GHz)	IL (dB)	RL (dB)	Controllable bandwidth	FBW %	Isolation (Tzs)/Rejection band (GHz@dB)	Selectivity	Circuit area (λ_g^2)/(mm^2)
This work	2.5 / 4	0.42 / 0.56	25 / 25.4	Yes	8 / 5	1 / (3.6@20)	Good	0.028 / 91.7
[12]	4.3 / 8.6	6.1 / 1	15 / 15	No	45 / 14	2 / (4.5@20)	Poor	0.10 / 204.5
[6]	2.6 / 3.5	1.1 / 1.2	18 / 20	No	11 / 3.2	1 / (3@20)	Poor	0.0045 / 63
[9]	2.38 / 4.98	2.2 / 1	25 / 32	No	8 / 8.8	1 / (3@15)	Good	0.36 / 195.8
[10]	2.33 / 4.36	1.5 / 1.6	19 / 16	No	6 / 5.7	2 / (1.4@20)	Good	0.064 / 395
[7]	2.4 / 3.5	0.2 / 0.2	17 / 17	No	1.66 / 1.7	None / (1.6@20)	Good	0.015 / 56
[8]	2.4 / 5.2	0.3 / 0.7	22 / 20	Yes	52 / 23	2 / (1.4@20)	Poor	0.056 / 427

Tab. 2. Physical dimensions of the double-layered SL-SIR DB-BPF, Fig. 1 (a) and Fig. 2 (a).

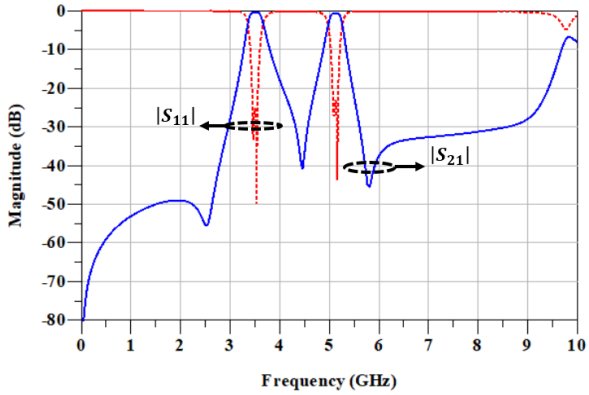

Fig. 7. The simulated $|S_{21}|/|S_{11}|$ magnitudes of the 3.5/5.2 GHz multi-layered SL-SIR dual-band BPF.

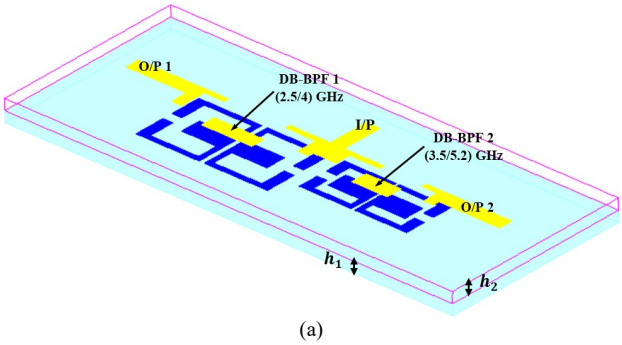

(a)

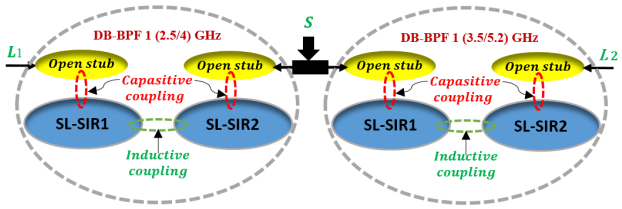

(b)

Fig. 8. The multi-layered quad-channel diplexer: (a) 3-D geometry of its conductor layout. (b) Coupling schematic diagram.

Dual-band SL-SIR BPF	Output port	Input port	Short open-stub
Filter 1 (2.5/4) GHz	ℓ_{w1} = 2 mm, ℓ_{w2} = 3 mm	ℓ_{w1} = 3 mm, ℓ_{w2} = 2.5 mm	ℓ_4 = 5 mm, w_4 = 1.4 mm
Filter 2 (3.5/5.2) GHz	ℓ_{w1} = 1.5 mm, ℓ_{w2} = 2 mm	ℓ_{w1} = 3 mm, ℓ_{w2} = 2 mm	ℓ_4 = 3.5 mm, w_4 = 1.6 mm

Tab. 4. The final tuned dimensions of the developed diplexer, Fig. 8 (a).

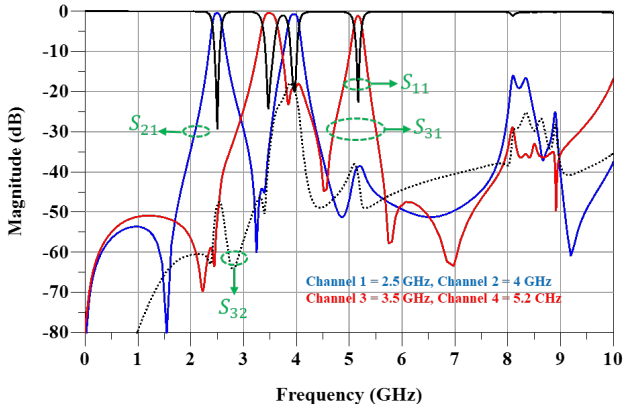

Fig. 9. The simulated S-parameters of the multi-layered SL-SIR diplexer: $|S_{21}|$, $|S_{31}|$, $|S_{11}|$ and $|S_{23}|$.

results are abundantly evident that the filter has a compact footprint excluding the I/O feeding ports covering only an area of 0.0639 λ_g^2 calculated at the lower BPF's center frequency. Also, the diplexer providing an isolation level of –20\–40 dB at the lower/upper bands and a wide spurious elimination capability of about 4.5 GHz at 15 dB. In addition, the filter selectivity is very good and the insertion losses and return losses of about (0.44/0.74) dB/ (0.45/1.12) dB and (21.30/21.72) dB / (19.81/20.54) dB over a 3-dB bandwidth of (175/195) MHz / (272/223) MHz at the diplexer out channels (2.5/4) GHz and (3.5/5.2) GHz, respectively.

To establish the developed diplexer Fig. 8(a), the planner's bottom and top diplexer circuits are individually manufactured using two substrates as shown in Fig. 10(a). Then the two circuits are integrated vertically using crystal bond mounting adhesives, Fig. 10(b). Finally, the diplexer responses are carried out with the assistance of an E5071C VNA and reported in Fig. 10(c) and (d).

A comparison between the attitudes obtained from the measurement and simulation can be found in Fig. 10(c) and (d).This figure suggests that these attitudes are reasonably matched one to another. In point of fact, this is most likely attributable to the manufacturing process, particularly the vertical feeding process. Nevertheless, the produced 3-port four-channel diplexer is compared with some recently works in Tab. 5. It is revealed that the proposed diplexer has compact size, wide rejection band, high selectivity, and flexible desired frequency allocation.

Ref.	Frequency (GHz)	Loads /Channels	Isolation (dB)	FBW %	IL (dB)	RL (dB)	Stopband (GHz)/Atten. (dB)	Selectivity	Circuit area: $(\lambda_g^2)/(mm^2)$
This work	2.5/4–3.5/5.2	2/4	≥ 20	8/5–8/5	0.44/0.74–0.45/1.12	21.302/21.724–19.816/20.542	5.5/15	Good	0.063/204
[19]	0.9/2.25–1.45/2.7	2/4	≥ 30	6.4/4.4–19/2.2	0.5/0.4–1.3/1.8	21/22–18/17	1/15	Poor	0.064/3167
[20]	2.15/3.6–2.72/5.05	2/4	≥ 28	8.17/3.6–5.9/4.4	0.81/1.43–1.32/0.90	16.34/21.2–19.65/16.37	0.6/10	Poor	0.0274/533.6
[18]	1.83/2.45–3.5/5.2	2/4	≥ 25	13/17.3–18.9/17.7	0.097/0.24–0.13/0.17/	28.2/19.2–20.9/26.2	0.5/15	Good	0.056/812
[21]	1.08/1.58–1.3/1.8	2/4	≥ 27	7/5.2–7.4/5.5	0.39/0.75–0.61/0.48	21.5/22.1–20.2/21.3	1/15	Good	0.058/972

Tab. 5. Comparison with recently reported quad-band diplexers.

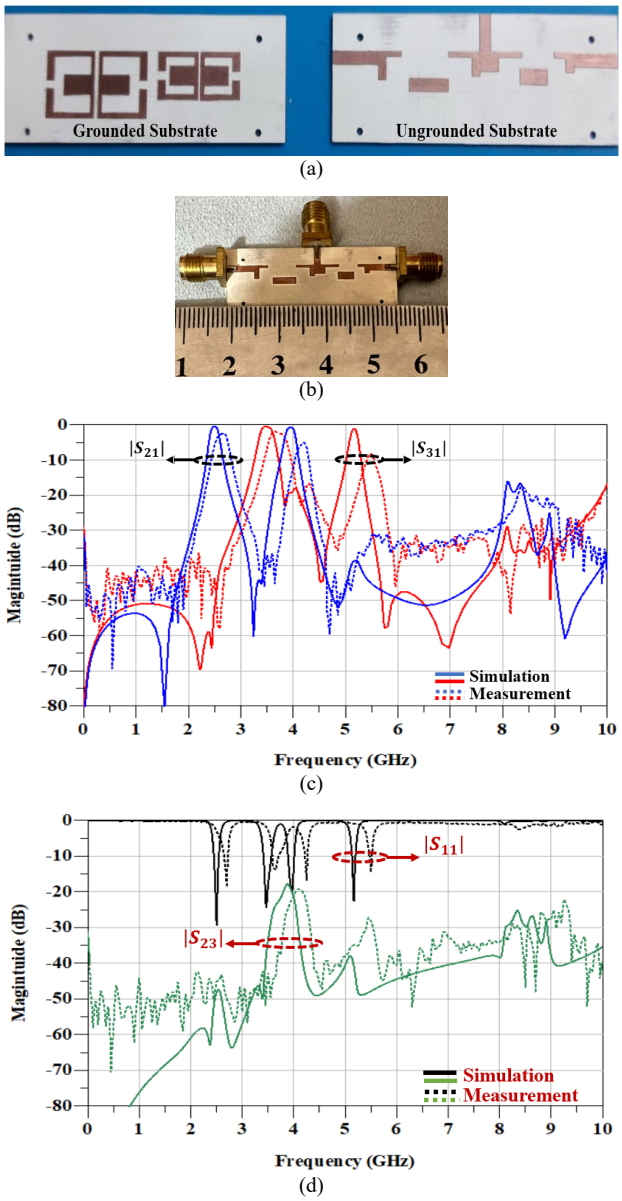

Fig. 10. The manufactured multi-layered SL-SIR diplexer, Fig. 8(a): (a) Photograpf befor alignment. (b) Photograph after alignment. (c) Its simulation and measurement scattering-parameters $|S_{21}|$ and$|S_{31}|$, and (d) Its simulation and measurement scattering-parameters $|S_{11}|$ and $|S_{23}|$.

4. Conclusion

Based on a multilayered SL-SIR, a distinguish design technique for developing a miniaturized dual-band BPF and quad-channel diplexer with wide out-of-band suppression characteristic has been presented in this paper. The SL-SIR is a dual-mode resonator. Therefore, its resonance characteristic was determined using even-odd analysis theory. The desired circuits of the suggested dual band BPF and the quad-band diplexer were realized and constructed on grounded and ungrounded substrates. To this end, 2.5/4 GHz dual-band BPF and 2.5/4–3.5/5.2 GHz diplexer were simulated, fabricated, and measured. A comparison between the simulated and measured results were discussed in deep. However, the developed filter circuits were significantly established with high filtering response characteristics in which the diplexer insertion/return losses are (0.44/0.74) dB/ (0.45/1.12) dB at channel 1/channel 2 and (21.30/21.72) dB/ (19.81/20.54) dB at channel 3/channel 4. Also, the diplexer has an ultra rejection band exceeding 5.5 GHz and a very compact surface area of 204 mm^2.

References

[1] HAMMED, R. T. Compact Marchand balun circuit for UWB application. *AEU-International Journal of Electronics and Communication*, 2015, vol. 69, no. 5, p. 851–855. DOI: 10.1016/j.aeue.2015.02.005

[2] CHOUDHARY, D. K., CHAUDHARY, R. K. Compact lowpass and dual-band bandpass filter with controllable transmission zero/center frequencies/passband bandwidth. *IEEE Transactions on Circuits and Systems: II Express Briefs*, 2020, vol. 67, no. 6, p. 1044–1048. DOI: 10.1109/TCSII.2019.2931446

[3] HAMMED, R. T. Miniaturized high-order ultra-wideband bandpass filters with multiple band rejection notches. *Electromagnetics,* 2015, vol. 35, no. 8, p. 538–549. DOI: 10.1080/02726343.2015.1101808

[4] TAN, Z., LU, Q.-Y., CHEN, J.-X. Differential dual-band filter using ground bar-loaded dielectric strip resonators. *IEEE Microwave and Wireless Components Letters,* 2019, vol. 30, no. 2, p. 148–151. DOI: 10.1109/LMWC.2019.2957980

[5] HAMMED, R. T., ABDUL-JABBAR, Z. M. Multilayered stepped impedance loaded-resonator for compact dual-band rejection filter design. *Electromagnetics*, 2017, vol. 37, no. 8, p. 493–499. DOI: 10.1080/02726343.2017.1392717

[6] DAO, X. P., NGUYEN, V. S., TRAN, V. D., et al. A compact dual bandpass filter using dual composite right-/left-handed and open-loop ring resonators for 4G and 5G applications. *Radioengineering*, 2024, vol. 33, no. 1, p. 213–221. DOI: 10.13164/re.2024.0213

[7] HAMMED, R. T., ABBAS, S. M. A small dual narrowband BPF with ultra-rejection band using grounded stepped-impedance resonator. *IETE Journal of Research*, 2023, vol. 69, no. 5, p. 2811–2816. DOI: 10.1080/03772063.2021.1906337

[8] LIANG, G.-Z., CHEN, F.-C. A compact dual-wideband bandpass filter based on open-/short-circuited stubs. *IEEE Access*, 2020, vol. 8, p. 20488–20492. DOI: 10.1109/ACCESS.2020.2968518

[9] CHANG, H., SHENG, W., CUI, J., et al. Multilayer dual-band bandpass filter with multiple transmission zeros using discriminating coupling. *IEEE Microwave and Wireless Components Letters,* 2020, vol. 30, no. 7, p. 645–648. DOI: 10.1109/LMWC.2020.2995181

[10] LI, D., WANG, J., LIU, Y., et al. Selectivity-enhancement technique for parallel-coupled SIR based dual-band bandpass filter. *Microwave and Optical Technology Letters,* 2021, vol. 63, no. 3, p. 787–792. DOI: 10.1002/mop.32672

[11] KISHORE, S., ARORA, A, PHANI KUMAR, K. V., et al. Compact dual-band bandpass filter with high-passband isolation using coupled lines and open stub. *IEEE Microwave and Wireless Components Letters*, 2021, vol. 63, no. 11, p. 2710 to 2714. DOI: 10.1002/mop.32940

[12] KARIMI, G., AMIRIAN, M., LALBAKHSH, A., et al. A new microstrip coupling system for realization of a differential dual-band bandpass filter. *AEU-International Journal of Electronics and Communications*, 2019, vol. 99, p. 186–192. DOI: 10.1016/j.aeue.2018.11.004

[13] SHAHEEN, M. M., MAHMOUD, N. M., ALI, M. A., et al. Implementation of a highly selective microstrip diplexer with low insertion loss using square open-loop resonators and a T-junction combiner. *Radioengineering*, 2022, vol. 31, no. 3, p. 357–361. DOI: 10.13164/re.2022.0357

[14] YANG, L., GÓMEZ-GARCÍA, R. Multilayer microstrip closely-spaced-channel wideband diplexer with highly selective fourth-order filtering responses. *IEEE Transactions on Circuits and Systems: II Express Briefs*, 2022, vol. 69, no. 9, p. 3769–3773. DOI: 10.1109/TCSII.2022.3173910

[15] NWAYANA, A. O., YEO, K. S. K. Microwave diplexer purely based on direct synchronous and asynchronous coupling. *Radioengineering,* 2016, vol. 25, no. 2, p. 247–252. DOI: 10.13164/re.2016.0247

[16] HAMMED, R. T. Multilayered U-shape diplexer for high performance multifunctional wireless communication systems. *AEU-International Journal of Electronics and Communications*, 2022, vol. 150, p. 1–5. DOI: 10.1016/j.aeue.2022.154217

[17] CHEN, C.-F., LIN, C.-Y., TSENG, B.-H., et al. A compact microstrip quad-channel diplexer with high-selectivity and high-isolation performances. In *IEEE MTT-S International Microwave Symposium (IMS2014)*. Tampa (FL, USA), 2014, p. 1–3. DOI: 10.1109/MWSYM.2014.6848271

[18] YAHYA, S. I., NOURI, L. A low-loss four-channel microstrip diplexer for wideband multi-service wireless applications. *AEU-International Journal of Electronics and Communications*, 2021, vol. 133, p. 1–7. DOI: 10.1016/j.aeue.2021.153670

[19] CHEN, C. F., WANG, G. Y., LI, J. J. Compact microstrip dual-band bandpass filter and quad-channel diplexer based on quintmode stub-loaded resonators. *IET Microwaves, Antennas and Propagation,* 2018, vol. 12, no. 12, p. 1913–1919. DOI: 10.1049/iet-map.2018.0079

[20] ZHANG, J., PANG, D., WANG, W., et al. Microstrip quad-channel diplexer using quad-mode square ring resonators. *IEEE Microwave and Wireless Components Letters*, 2019, vol. 61, no. 8, p. 2003–2007. DOI: 10.1002/mop.31827

[21] DEL RÍO, J. L M., FERNÁNDEZ-PRIETO, A., MARTEL, J., et al. Compact multilayered balanced-to-balanced dual-and tri-band diplexers based on magnetically coupled open-loop resonators. *IEEE Access*, 2022, vol. 10, p. 125435–125444. DOI: 10.1109/ACCESS.2022.3225542

[22] MAKIMOTO, M., YAMASHITA, S. *Microwave Resonators and Filters for Wireless Communication: Theory, Design and Application.* Berlin (Germany): Springer, 2010. DOI: 10.1007/978-3-662-04325-7

[23] AGILENT TECHNOLOGIES. *Advanced Design System (ADS)*. Palo Alto (CA, USA), 2016.

[24] HAMMED, R. T. Miniaturized dual-band bandpass filter using E-shape microstrip structure. *AEU-International Journal of Electronics and Communications*, 2015, vol. 69, no. 11, p. 1667 to 1671. DOI: 10.1016/j.aeue.2015.08.003

About the Authors ...

Soaad L. AJEEL was born in 1994. She received her B.Sc. in Electrical Engineering from the University of Technology-Iraq in 2018. She is currently a master's student in Electronic and Communication Engineering in the Department of Electrical Engineering, University of Technology-Iraq. Her research is microwave filter passive filters and diplexers.

Raaed T. HAMMED was born in 1973. He received his B.Sc. in Electrical and Electronic Engineering and his M.Sc. in Electronic Engineering from the University of Technology-Iraq in 1996 and 2002, respectively, the Ph.D. in Electronic/Microwave Engineering from the University of Essex/Colchester-UK in 2012. For the last four months in 2012, he was a researcher at the University of Essex. He is currently a Professor with the Department of Electrical Engineering, University of Technology-Iraq. He is a professional expert in fabrication process for single and double layer microstrip circuits. His research interest is in microwave passive and active circuits such as filters, balun circuit, diplexers, power amplifier, and etc.